



This is a repository copy of *Quantifying the effects of climate and environmental changes on evapotranspiration variability in the Sahel*.

White Rose Research Online URL for this paper:

<https://eprints.whiterose.ac.uk/216355/>

Version: Accepted Version

Article:

Nkiaka, E., Bryant, R.G. orcid.org/0000-0001-7943-4781, Dembélé, M. et al. (3 more authors) (2024) Quantifying the effects of climate and environmental changes on evapotranspiration variability in the Sahel. *Journal of Hydrology*, 642. 131874. ISSN 0022-1694

<https://doi.org/10.1016/j.jhydrol.2024.131874>

© 2024 Elsevier B.V. The Authors. Except as otherwise noted, this author-accepted version of a journal article published in *Journal of Hydrology* is made available via the University of Sheffield Research Publications and Copyright Policy under the terms of the Creative Commons Attribution 4.0 International License (CC-BY 4.0), which permits unrestricted use, distribution and reproduction in any medium, provided the original work is properly cited. To view a copy of this licence, visit <http://creativecommons.org/licenses/by/4.0/>

Reuse

This article is distributed under the terms of the Creative Commons Attribution (CC BY) licence. This licence allows you to distribute, remix, tweak, and build upon the work, even commercially, as long as you credit the authors for the original work. More information and the full terms of the licence here:

<https://creativecommons.org/licenses/>

Takedown

If you consider content in White Rose Research Online to be in breach of UK law, please notify us by emailing eprints@whiterose.ac.uk including the URL of the record and the reason for the withdrawal request.



eprints@whiterose.ac.uk
<https://eprints.whiterose.ac.uk/>

Quantifying the effects of Climate and Environmental changes on Evapotranspiration Variability in the Sahel

Elias Nkiaka¹, Robert G. Bryant¹, Moctar Dembélé^{2,3}, Roland Yonaba⁴, Aigbedion Imuwahen
Priscilla⁵, Harouna Karambiri⁴

¹Department of Geography, University of Sheffield, Sheffield, S10 2TN, UK

²International Water Management Institute (IWMI), CSIR Campus, 6 Agostino Neto Road, Accra,
Ghana

³School of Geography and the Environment, University of Oxford, South Parks Road, Oxford
OX1 QY, UK

⁴Laboratory of Water, Hydro-Systems and Agriculture (LEHSA), International Institute for Water
and Environmental Engineering (2iE), 01 PO Box 594, Ouagadougou 01, Burkina Faso

⁵Department of Cartography and GIS, Federal School of Surveying, Oyo, Nigeria, P.M.B 1024
Oyo State, Nigeria

Elias Nkiaka (Corresponding author): e.nkiaka@sheffield.ac.uk

Corresponding author postal Address: Department of Geography, University of Sheffield,
Sheffield, S10 2TN, UK

Highlights:

- Significant increasing trends in annual ET in most parts of the Sahelian belt.
- Precipitation, humidity, and vapour pressure (climatic factors), and soil moisture and NDVI (environmental factors) are the most important variables controlling increase in ET.
- Vapour pressure has the highest positive elasticity score (2.58) while net radiation has the highest negative elasticity score (-9.58) on ET.
- The study covers the whole Sahelian belt from west to east making it to stand out from previous studies in the region that cover mostly the western Sahel.

26 **Abstract**

27 Whilst considerable research has been carried out to understand the effects of reforestation on
28 evapotranspiration (ET), such studies are generally absent in the Sahel even though the region is
29 currently undergoing extensive reforestation to halt desertification and land degradation. The
30 objective of this study is to identify and quantify the dominant climatic and environmental factors
31 influencing ET variability in the Sahel. However, achieving this goal in the Sahel is hindered by a
32 lack of in situ monitoring data. To overcome this challenge, this study adopts geospatial datasets
33 along with analytical methods to assess the climatic and environmental factors affecting ET in 45
34 watersheds in the Sahel over a period of four decades (1982-2021). Analyses show significant
35 increasing trends in annual ET in more than 90% of the watersheds. Precipitation and mean
36 temperature show significant increasing trends in all watersheds while windspeed, vapour pressure,
37 solar radiation, specific humidity, and atmospheric evaporative demand show mixed results with
38 both increasing and decreasing trends in different watersheds. Environmental variables including
39 soil moisture, and vegetation cover measured using the normalised difference vegetative index
40 (NDVI) also show consistent increasing trends in all watersheds. Statistical analyses further show
41 that climatic and environmental factors contribute about 80% of ET variance. The relative
42 contribution of climatic variables on ET variance is 75.11% while that of environmental variables
43 is 24.71%. This suggests that climatic factors have a higher influence on ET variability than
44 environmental factors. Analyses using the double logarithm elasticity model show that vapour
45 pressure has the highest positive elasticity coefficient (2.58) on ET while net radiation has the
46 highest negative elasticity coefficient (-9.58). This is the first study to cover the whole Sahelian belt
47 from west to east and the results may be crucial for adopting climate-smart reforestation policies,
48 enhance regional water management and improve our knowledge of vegetation-hydrology-climate
49 interactions in the Sahel.

50 **Keywords:** analytical methods; elasticity concept; partial correlation coefficient, least square and
51 double logarithm elasticity models; great green wall initiative; NDVI.

52 **1. Introduction**

53 Due to increased vulnerability caused by climate change and population growth, many dryland areas
54 are exposed to desertification and land degradation risk and ensuing contradiction between humans
55 and land (Sun *et al.*, 2023). To achieve land degradation neutrality -which is one of the sustainable
56 development goals (SDGs) and enhance carbon sequestration, many dryland areas are undergoing
57 extensive reforestation/afforestation (Arneth *et al.*, 2021; Schulze *et al.*, 2021). Considering the
58 vulnerability of the Sahel to desertification and land degradation (Mbow *et al.*, 2017), the region is
59 currently undergoing vast reforestation through the Great Green Wall Initiative (GGWI) (Mbow,
60 2017). The objective of the GGWI is to restore 100 million hectares of degraded land through
61 reforestation, sequester 250 million tons of carbon and create 10 million green jobs by 2030 (Mbow,
62 2017; Goffner *et al.*, 2019). Whilst many studies have been conducted in other regions undergoing
63 reforestation to understand the factors influencing actual evapotranspiration (ET) variability
64 (Teuling *et al.*, 2019; Yang *et al.*, 2022; Zheng *et al.*, 2022), such studies are generally lacking in
65 the Sahel. ET is an important component of regional energy cycle representing the complex
66 interaction between vegetation, climate, and landscape characteristics (Zhang *et al.*, 2019; Yang *et*
67 *al.*, 2021). It is also an important component of the water cycle with a strong influence on runoff
68 and soil moisture availability and groundwater recharge (Guo *et al.*, 2017; Yinglan *et al.*, 2019;
69 Condon *et al.*, 2020). Therefore, to achieve consistent, evidence-based allocation and management
70 of water resources in the context of the GGWI, it is crucial to identify and quantify the climatic
71 (abiotic) and environmental (biotic) factors influencing ET variability in the Sahel. Such information
72 may be crucial for adopting climate-smart reforestation policies to support the implementation of
73 the GGWI, enhance water management given the strong links between water scarcity and violent
74 conflicts in the Sahel (Nkiaka *et al.*, 2024) and improve our knowledge of vegetation-hydrology-
75 climate interactions in the Sahel.

76 Several studies have assessed the climatic and environmental factors influencing ET
77 variability at different scales. For example, Feng *et al.* (2020) showed that ET is strongly influenced

78 by precipitation at the global scale, while potential evapotranspiration, terrestrial water storage, and
79 catchment characteristics influence ET variability in energy-limited environments, arid and humid
80 regions respectively. Yang *et al.* (2022) reported that precipitation, temperature, and vegetation
81 cover are the dominant factors influencing ET variability in northwest China. Li *et al.* (2022) found
82 that precipitation, net radiation, and vapour pressure deficit exert greater control on ET variability
83 in dry climates, tropical regions, and boreal mid-latitude regions respectively. Land use change,
84 precipitation, and potential evapotranspiration were found to be the main factors influencing
85 evapotranspiration across Europe (Teuling *et al.*, 2019). Changing precipitation patterns and land
86 cover have been reported to be the dominant factors affecting the components of the hydrological
87 cycle in the Amazon (Heerspink *et al.*, 2020).

88 Different approaches have been used to study the effects of climatic and environmental
89 factors influencing ET. For example, Zheng *et al.* (2022) used the partial least squares structural
90 equation model to explore the relationship between ET and climatic and environmental factors.
91 Other studies adopted the Budyko framework (Teuling *et al.*, 2019; Feng *et al.*, 2020; Li *et al.*,
92 2022), the elasticity concept (Wang *et al.*, 2020; Yang *et al.*, 2022) and the complementary
93 relationship (Brutsaert, 2015; Li *et al.*, 2021) to analyse the effects of climate and vegetation changes
94 on ET. Adeyeri and Ishola (2021) applied the time-frequency wavelet decomposition method and
95 partial correlation analysis to reveal the factors influencing ET in West Africa. Ndehedehe *et al.*
96 (2018) used the independent component analysis to explore ET dynamics in sub-Saharan Africa.
97 Overall, most of the methods used for studying the relationship between ET and climatic and
98 environmental factors are data-driven analytical methods. Analytical methods use mathematical
99 equations based on the assumption that the catchment water balance remains under steady-state over
100 a long period of time (Dey and Mishra, 2017; Zhang *et al.*, 2023). Advantages of analytical methods
101 include: (1) simple model structure and (2) require minimum input data to produce results that are
102 practically useful for most hydrological applications (Hasan *et al.*, 2018).

103 Despite the high sensitivity of Sahelian vegetation to climate variability and environmental
104 change (Leroux *et al.*, 2017), very few studies have investigated the factors influencing ET
105 variability in the Sahel while existing studies have focused mostly on the western Sahel. Meanwhile,
106 the effects of vegetation on ET are conspicuously ignored in exiting studies. For example, Adeyeri
107 and Ishola (2021) showed that precipitation and atmospheric evaporative demand (AED) had a
108 greater influence on ET in the western Sahel. Ndiaye *et al.* (2021) revealed that ET in the western
109 Sahel is more sensitive to relative humidity, maximum temperature, and solar radiation. Ndehedehe
110 *et al.* (2018) attributed ET variability in the western Sahel to changes in precipitation, soil moisture
111 and temperature. The limited number of studies addressing this issue in the Sahel suggests that there
112 is a dearth of knowledge on the vegetation-hydrology-climate interactions which hampers the
113 development of climate-smart reforestation practices in the context of the GGWI and regional water
114 management. To overcome the challenge of widespread in situ data scarcity in the region, this study
115 leverages on the availability of a wide range of satellite-derived and reanalysis data. The main
116 advantage of such data is that they can provide high spatial resolution and long-term homogeneous
117 data for previously unmonitored regions at scales that are suitable for studying changes in the
118 hydrological cycle (Sheffield *et al.*, 2018).

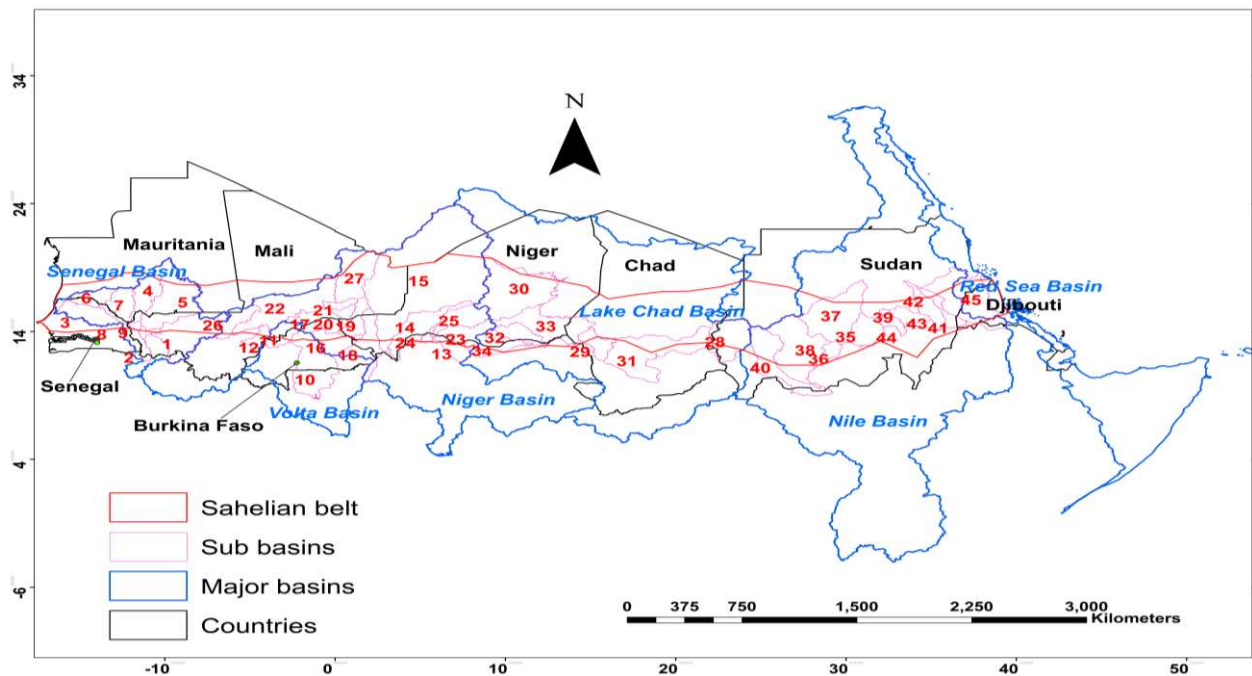
119 From the above, the objectives of this study are to: (1) analyse trends in annual ET, climatic
120 and environmental (soil moisture and vegetation cover) variables, (2) identify the main climatic and
121 environmental factors influencing ET and, (3) quantify the impact of climate and vegetation changes
122 on ET across the Sahel.

123 **2. Materials and Methods**

124 **2.1. Study area.**

125 The Sahel stretches from Senegal to Eritrea with a length of about 8,000 km. It is a transitional zone
126 located between the Sahara Desert to the north and the Sudanian-savanna to the south covering ten
127 countries with a population of about 150 million (Figure 1). It is one of the world's largest water-
128 limited environments and ranked amongst the most fragile ecosystems in the world (Ghins *et al.*,

129 2022). The Sahel is remarkable because of a mega drought that affected the region from the 1970s
 130 to mid-1990 attracting much media coverage because of the humanitarian crisis that ensued from
 131 the drought (Nicholson *et al.*, 1998; Dai *et al.*, 2004). Precipitation estimates from Climate Hazards
 132 Group InfraRed Precipitation with Station data (CHIRPS) over four decades (1982-2021) show that
 133 annual precipitation varies from 71-200 mm/year in the north to about 700-1000 mm/year in the
 134 south. The present study covers 45 watersheds nested within six major hydrological basins including
 135 Senegal, Volta, Niger, Lake Chad, Nile, and Red Sea (Figure 1). The total surface area covered by
 136 all the watersheds is about 3,021,412 km² ranging in size from 4095 km² (Senegal 4) to 541,267 km²
 137 (Dallol Bosso). Most of the watersheds lie between Latitudes 12°N and 20°N. A full list of the
 138 watersheds and their characteristics is available in Appendix A. Shapefiles of the watersheds are
 139 collected from HydroSHEDs which provides a seamless global coverage of consistently sized and
 140 hierarchically nested sub-basins using the high-resolution Shuttle Radar Topographic Mission
 141 digital elevation model (Lehner and Grill, 2013). HydroSHEDs shapefiles have been used in several
 142 studies e.g., (Gebrechorkos *et al.*, 2022; Zhang *et al.*, 2023; Nkiaka and Okafor, 2024).



143
 144 Figure 1: Map of the study region showing the different countries, major hydrological basins, and
 145 nested sub-basins and the Sahelian belt. Sub-basins are numbered from left to right. A full list of the
 146 sub-basins and their characteristics is available in Appendix 1.

147 **2.2. Data and aggregation**

148 Table 1 summarises the characteristics of the different datasets used in the study. The ET data used
 149 in the study has been validated in previous studies e.g., (Nkiaka *et al.*, 2022) and also used in several
 150 studies in the Sahel e.g., (Gbohoui *et al.*, 2021; Hernández *et al.*, 2021). CHIRPS, AgERA5, GLEAM
 151 Soil moisture and NDVI data from MODIS have been validated and also used extensively in other
 152 studies in the region e.g., (Fensholt *et al.*, 2009; Wang *et al.*, 2023; Asante *et al.*, 2022; Dembélé *et*
 153 *al.*, 2020). A complete description of the different datasets is available in their respective references
 154 provided in Table 1.

155 Table 1: Characteristics of products and data used in the study.

Variable type	Product name and reference	Spatial resolution	Temporal resolution
Sub-basin (km ²)	HydroSHEDs, (Lehner and Grill, 2013)	-	-
Precipitation	CHIRPS (Funk <i>et al.</i> , 2015)	0.05°	Daily
Evapotranspiration (ET)	TerraClimate (Abatzoglou <i>et al.</i> , 2018)	0.041°	Monthly
Atmospheric evaporative demand (AED)	TerraClimate (Abatzoglou <i>et al.</i> , 2018)	0.041°	Monthly
Mean temperature	AgERA5 (Boogaard, 2020)	0.1°	Daily
Solar radiation		0.1°	Daily
Windspeed		0.1°	Daily
Vapour pressure		0.1	Daily
Specific humidity	CFSR (Saha <i>et al.</i> , 2014)	0.19°	Daily
Soil moisture (0-100 cm)	GLEAM (Martens <i>et al.</i> , 2017)	0.25°	Daily
Vegetation cover (NDVI)	MOD13A1 V6 (Didan, 2015)	500m	16 days

156
 157 The climatic and environmental variables were downloaded at annual timescale at their respective
 158 native spatial resolutions using the Climate Engine research App [<https://app.climateengine.com>]
 159 (Huntington *et al.*, 2017). Watersheds shapefiles can be uploaded to Climate Engine directly from a
 160 computer folder or using the Google Earth Engine interface through a custom user account. Soil
 161 moisture data are downloaded from GLEAM and processed using OriginPro software. All the data
 162 were downloaded as spatial average over each watershed.

163

164

2.3. Trend analyses

The non-parametric Mann-Kendall test and Sen's slope estimator are used respectively for trend analysis and to quantify trend magnitude and significance. The Mann-Kendall test and Sen slope estimator are widely used for detecting the presence of statistically significant increasing or decreasing trends in hydroclimatic time series and have been used in several studies in the region e.g., (Nkiaka *et al.*, 2017). Although several different Mann-Kendall tests exist, e.g., (Güçlü, 2020), the study adopted the classical Mann-Kendall test. The period 1982–2021 is adopted for climate variables while 2000–2021 is used for vegetation change (NDVI). Trend analyses are conducted at the 5% significance level.

2.4. Identifying the factors influencing evapotranspiration (ET) variability

The study uses three statistical methods to assess the factors influencing ET in the Sahel. Considering that collinearity and interactions among the different independent variables cannot be overlooked, partial correlation coefficient (PCC) is used to determine the relationship between each independent variable (climate and environmental variables) and the dependent variable (ET) while controlling for the effects of all the other independent variables. PCC is calculated using the following equation (Engström and Ekman, 2010) and has been used in several studies e.g., (Yang *et al.*, 2022; Adeyeri and Ishola, 2021).

$$\rho_{X,ET(Y)} = \frac{\rho_{X,ET} - \rho_{X,Y}\rho_{Y,ET}}{\sqrt{1 - \rho_{X,Y}^2}\sqrt{1 - \rho_{Y,ET}^2}} \quad (1)$$

Where $\rho_{X,ET(Y)}$ is the partial correlation coefficient between X & ET considering the effect of variable Y; $\rho_{X,ET}$ and $\rho_{Y,ET}$ are the correlation coefficients between ET and X & Y, respectively, and $\rho_{X,Y}$ is the correlation coefficient between X and Y. In the second step, Pearson correlation was used to establish how change in the independent variable affects the dependent variable. In the third step, multiple linear regression analysis is conducted between the rate of change of each independent variable and the rate of change of the dependent variable to determine the relative contributions of each independent variable on the dependent variable. This was achieved using multivariable

190 regression at 5% significance level using equation (2). The relative contributions of the change in
191 each independent variable to the rate of change in ET was then estimated from the multivariable
192 regression coefficients using equation (3). Equations (2) and (3) have been used in several previous
193 studies to estimate the relative contribution of independent variables on the dependent variable e.g.,
194 (Chen *et al.*, 2022; Yang *et al.*, 2022).

$$195 \quad Y = aX_1 + bX_2 + cX_3 + \dots dX_n \quad (2)$$

$$196 \quad r_x = \frac{|a|}{|a| + |b| + |c| + \dots |d|} \times 100\% \quad (3)$$

197 Where Y is the standardized dependent variable (ET), X_1 , X_2 , X_3 , and X_n are the standardized
198 independent variables (precipitation, soil moisture, mean temperature, windspeed, net radiation,
199 humidity, vapour pressure, AED and NDVI); r_x is the relative contribution of each independent
200 variable to ET and a , b , c , \dots & d are the regression coefficients of the independent variables.

201 **2.5. Quantifying the effects of climate and vegetation changes on evapotranspiration.**

202 Analytical method based on the Elasticity concept was used to quantify the effect of climate and
203 vegetation changes on ET.

204 **2.5.1. Attribution of ET change**

205 The elasticity concept is useful for quantifying how a relative change in one variable affects the
206 other variable (Ahiablame *et al.*, 2017; Tan *et al.*, 2020). The elasticity concept is widely used in
207 hydrology due to its clear physical meaning and simple formulation (Sankarasubramanian *et al.*,
208 2001). Due to its limited input data requirements, the elasticity concept has been extended to
209 investigate the sensitivity of runoff, baseflow and ET to climate and vegetation changes (Ahiablame
210 *et al.*, 2017; Chen *et al.*, 2022; Tan *et al.*, 2020). Since its original formulation, several other
211 elasticity models have been proposed such as the least square elasticity model (Zheng *et al.*, 2009),
212 the multivariable double logarithm, and multivariable transformation analyses models (Tsai, 2017).
213 This study adopts two elasticity models: (1) the least square elasticity (LSE) model because it can
214 overcome the problem associated with small sample size and (2) the double logarithm elasticity

215 (DLE) model which has previously been used exclusively for quantifying the impact of climate and
 216 vegetation changes on streamflow (Tsai, 2017; Khan *et al.*, 2022). The aim of using the two elasticity
 217 models is to ensure that our results are robust.

218 The LSE model is expressed as:

$$219 \quad \varepsilon = \frac{\bar{X}}{\overline{ET}} \cdot \frac{\sum(X_i - \bar{X})(ET_i - \overline{ET})}{\sum(X_i - \bar{X})^2} = \rho_{X,Q} \cdot C_Q / C_X \quad (4)$$

220 Where ET is evapotranspiration and X represent the annual climate or environment variable
 221 (precipitation, soil moisture, mean temperature, solar radiation, windspeed, specific humidity, AED
 222 and NDVI) and \bar{X} and \overline{ET} represent the multiyear annual mean climatic/environmental variable and
 223 ET values respectively. $\rho_{X,Q}$ is the correlation coefficient between the climatic/environment variable
 224 and ET and C_X and C_{ET} are coefficients of variation of climatic and environmental variables and ET,
 225 respectively.

226 The DLE model is built on the premise that evapotranspiration (ET) is influenced by multiple factor
 227 elasticities in the form of regression coefficients of a multivariable regression model. The
 228 multivariable function describing the influence of climatic and environmental variables on ET is
 229 expressed as:

$$230 \quad ET = f(P, SM, T, H, S, W, VP, AED, NDVI) \quad (5)$$

231 Where $P, SM, T, H, S, W, VP, AED, NDVI$ represent precipitation, soil moisture, mean temperature,
 232 solar radiation, windspeed, specific humidity, AED and NDVI. We then modify equation (5) using
 233 the approach proposed by Tsai (2017) as follows:

$$234 \quad ET = P^{\beta_1} SM^{\beta_2} T^{\beta_3} H^{\beta_4} S^{\beta_5} W^{\beta_6} VP^{\beta_7} AED^{\beta_8} NDVI^{\beta_9} \quad (6)$$

235 Taking logarithm of both sides of equation (6) produces the following equation:

$$236 \quad \text{Log}ET = \beta_1 \text{Log}P + \beta_2 \text{Log}SM + \beta_3 \text{Log}T + \beta_4 \text{Log}H + \beta_5 \text{Log}S + \beta_6 \text{Log}W + \beta_7 \text{Log}VP + \beta_8 \text{Log}AED + \beta_9 \text{Log}NDVI \quad (7)$$

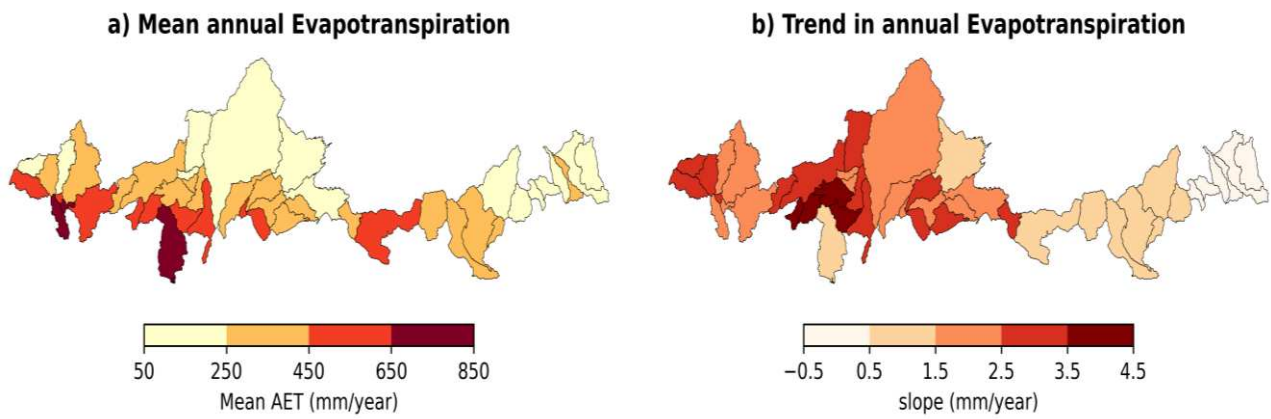
237 Where β_n is the elasticity coefficient of the different climatic and environmental variables. In our
238 approach, we estimated the elasticity coefficient of each independent variable on ET separately. The
239 elasticities are then estimated as coefficients of the ordinary least squares (OLS) regression analysis
240 between ET and each of the independent variables. In running the regression analysis, the intercept
241 term was left unadjusted (i.e., assumed to be zero).

242 After estimating the elasticity coefficients using the two methods, we used linear correlation
243 analysis to measure the strength of the relationship between the elasticity coefficients obtained using
244 the two models. To determine which elasticity model to be adopted for further analysis and
245 interpretation, we conducted a linear regression analysis between ET and the different independent
246 variables. We conducted the same analysis for their log-transformed counterparts (ET and climatic
247 and environmental variables). Lastly, we used the adjusted R^2 values obtained from both linear
248 regression models to assess the regression goodness of fit for the log transformed and least square
249 elasticity models (Tsai, 2017; Khan *et al.*, 2022). We adopted the adjusted R^2 because it provides a
250 better overall performance of a regression model by considering the number of predictors in the
251 model. We estimated the mean of the adjusted R^2 obtained from both models and adopted the model
252 with highest mean adjusted R^2 .

253 **3. Results**

254 **3.1. Trend analysis**

255 Figure 2 shows the mean annual ET estimates and trends across Sahelian watersheds over a period
256 of 4 decades (1982 -2021). It can be observed that there is a strong spatial variability in mean annual
257 ET across the study area varying from 50-850 mm/year. High annual ET occur mostly in the
258 southern fringes of the Sahel while low annual ET occur in watersheds around the central and eastern
259 Sahel (Figure 2a). Trend analysis also shows a strong spatial heterogeneity with statistically
260 significant increasing trends visible around watersheds in the western and central Sahel (0.5-
261 4.5mm/year) and statistically significant decreasing trends observed in the far eastern Sahel (Figure
262 2b).



263

264

Figure 2: Mean annual ET (a) and trends in annual ET across the Sahelian belt.

265

266

267

268

269

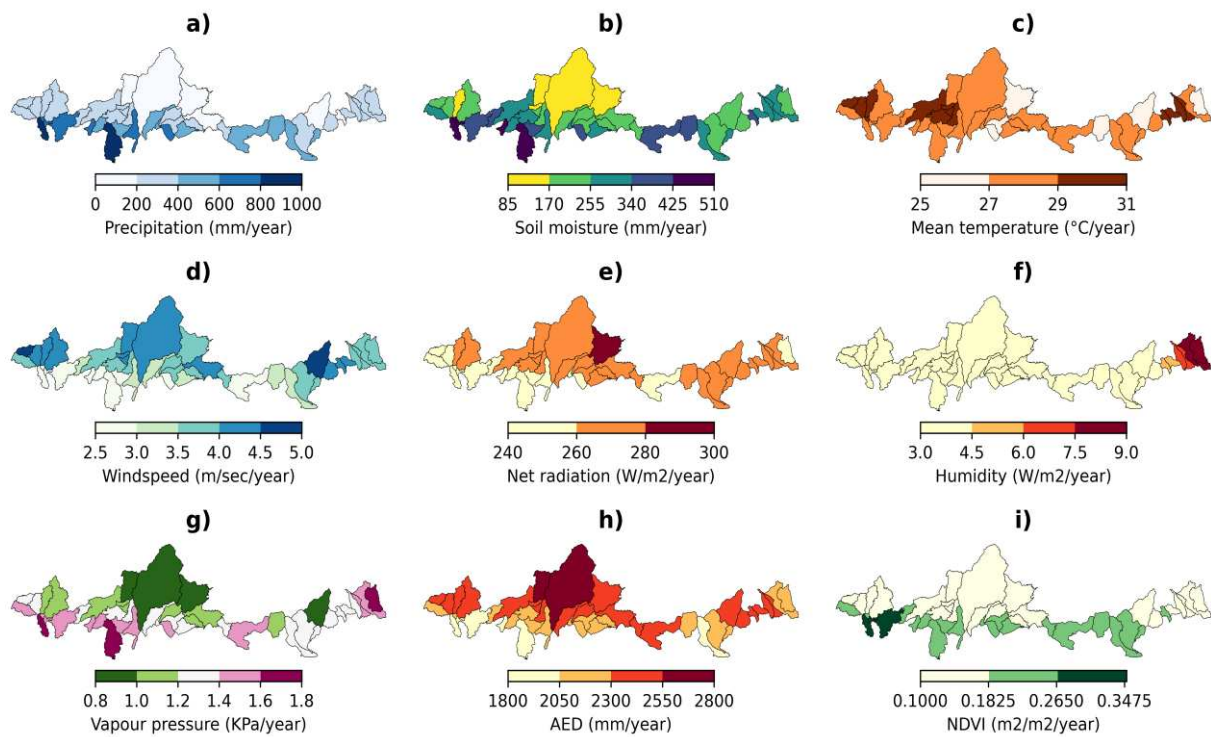
270

271

272

273

Mean annual estimates of all the climatic and environmental variables are shown in Figure 3. There is a strong spatial heterogeneity in precipitation and soil moisture across the study area (Figure 3a & b). Mean temperature is quasi uniform in the western and central Sahel but shows strong spatial heterogeneity in the eastern Sahel (Figure 3c). Windspeed and net radiation are higher in the northern Sahel compared to the south while relative humidity appears to be uniform across the region with a strong spatial heterogeneity observable around the far eastern Sahel (Figure 3d, e, & f). There is also a strong spatial heterogeneity in vapour pressure and AED across the study area (Figure 3g & h). NDVI scores are higher in watersheds located in the southern fringers of the Sahel compared to those in the north and eastern Sahel (Figure 3i)



274

275

Figure 3: Mean annual estimates of climate and environmental variables.

276

277

278

279

280

281

282

283

284

285

286

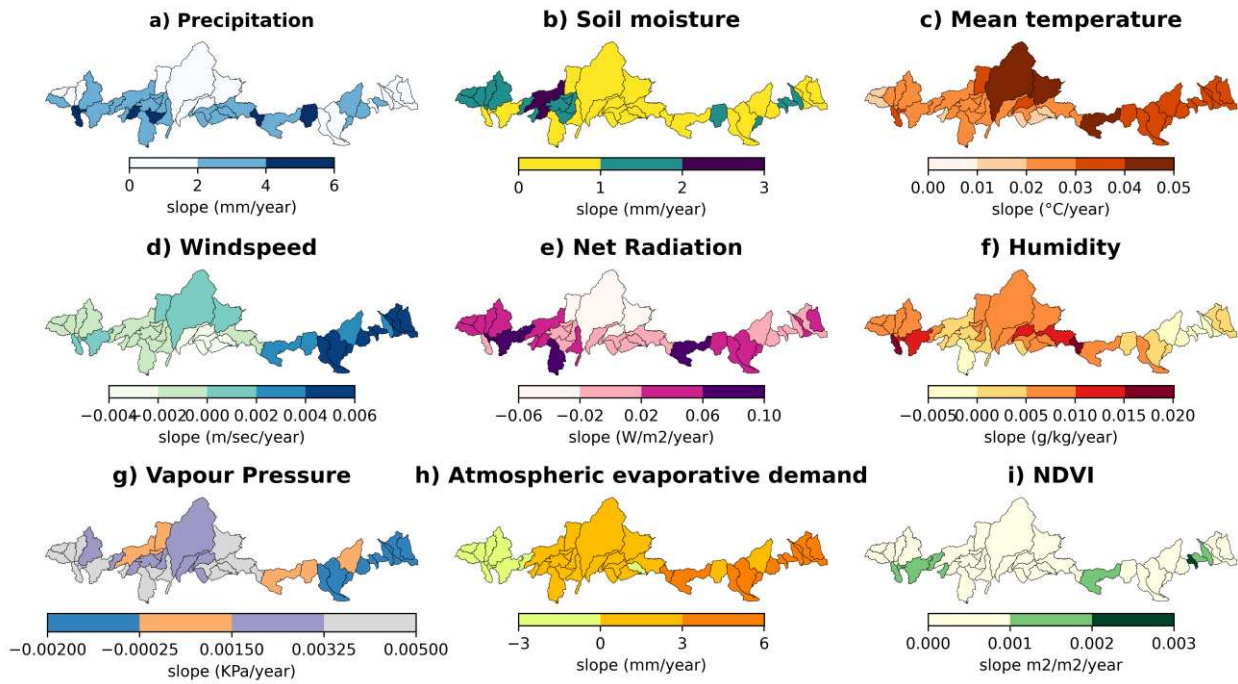
287

288

289

290

Figure 4 shows the results of trend analysis for all the other climatic variables over a period of four decades (1981-2021) and NDVI over two decades (2000-2021). Trend analyses show statistically significant increasing trends in annual precipitation, soil moisture and mean temperature across the region (Figure 4a, b & c). Other climate variables show both statistically significant increasing and decreasing trends, however, there is a strong spatial heterogeneity in trend magnitudes. For example, increasing and decreasing trends in windspeed are perceptible in the eastern Sahel and western Sahel respectively (Figure 4d). Decreasing trends in net radiation are also perceptible around the central Sahel (Figure 4e). Statistically significant increasing trends in specific humidity are visible in the western and central Sahel while decreasing trends occur in the eastern Sahel (Figure 4f). Decreasing trends in vapour pressure occur in the eastern Sahel while increasing trends are clearly visible in the central and western Sahel. There is also a strong spatial heterogeneity in AED trends with statistically significant increasing trends clearly visible in the eastern Sahel (6 mm/year) while statistically significant negative trends occur in the western Sahel. (Figure 4h). There is a consistent increase in NDVI across all watersheds with statistically significant trends occurring in a few watersheds (Figure 4i).



291

292 Figure 4: Trends in annual climatic variables and environmental variables across the Sahel

293 **3.2. Factors influencing ET.**

294 Table 2 shows the results of PCC between ET and each independent variable while controlling for
 295 the effect of all the other variables. PCC scores show that precipitation, mean temperature, net
 296 radiation, specific humidity, vapour pressure and NDVI have statistically significant correlations
 297 with ET. Results of Pearson correlation between the rate of change in each independent variable and
 298 the rate of change in the dependent variable (ET) are also available in Table 2 and in Figure 4.

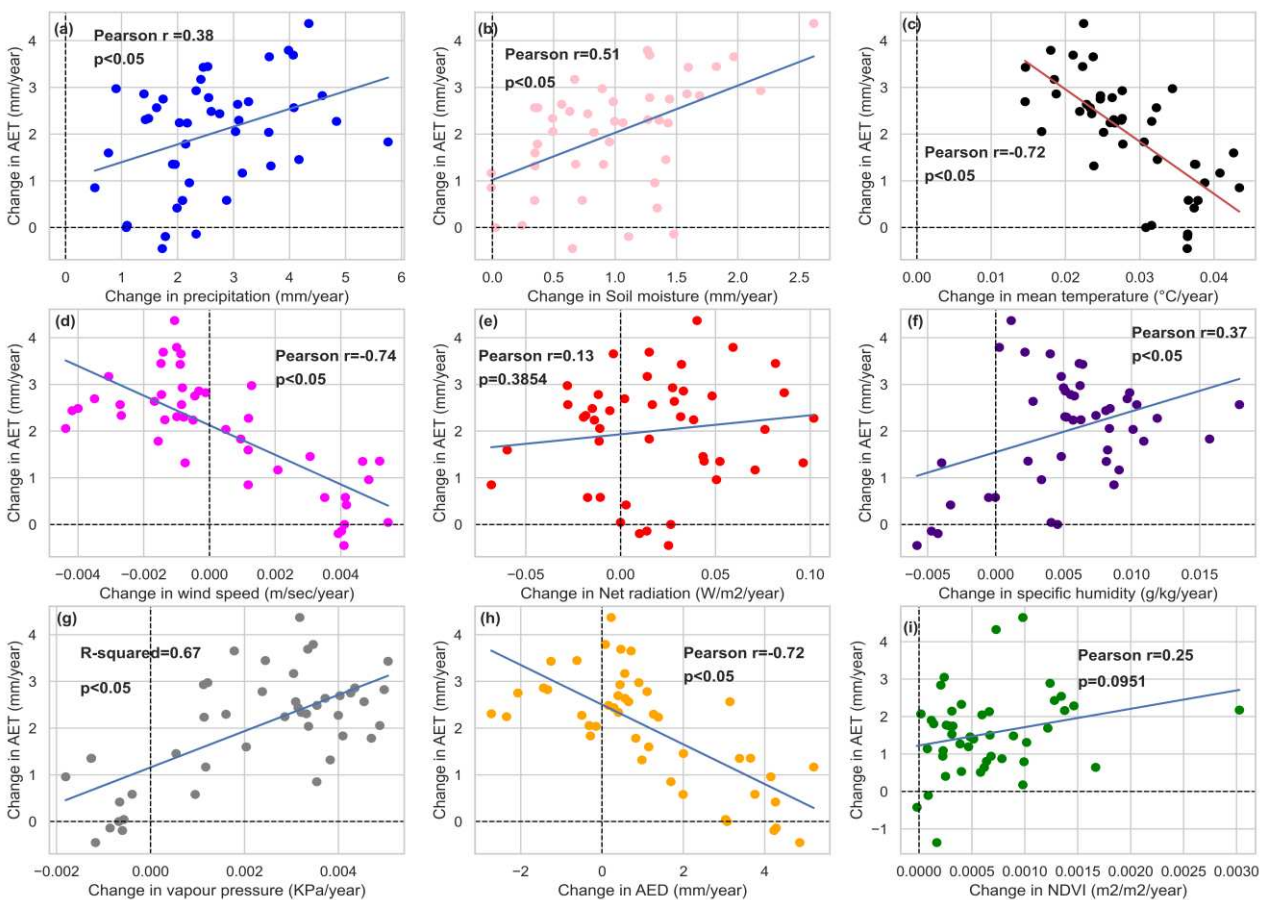
299 Table 2: Identifying the factors influencing ET variability.

Variable	Partial correlation	Pearson Correlation	Multivariable Regression	
			Relative weight	Relative contribution (%)
Precipitation	0.85**	0.38**	0.0367	4.61
Soil moisture	0.06	0.51**	0.1681	21.12
Mean temp	-0.35**	-0.72**	0.1225	15.39
Windspeed	-0.02	-0.74**	0.1629	20.46
Net radiation	-0.64**	0.13	0.5540	6.96
Humidity	0.71**	0.37**	0.0126	1.58
Vapour pressure	0.41**	0.67**	0.0994	12.39
AED	0.004	-0.72**	0.1093	13.72
NDVI	0.28*	0.25*	0.0292	3.67

300 ** Indicates statistically significant at 5% significance; *indicates statistically significant at 1%
 301 significance level.

302 Multivariable regression indicate that the independent variables contributed about 80% of the ET
 303 variance ($R^2=0.80$ and adjusted $R^2=0.75$). The relative contributions of soil moisture, mean

304 temperature, windspeed, AED and vapour pressure were 21.12%, 20.46%, 15.39%, 13.72% and
 305 12.49% respectively suggesting that these are the main variables influencing ET in the Sahel (Table
 306 2). Pearson correlation analysis also indicate that a positive change in precipitation, soil moisture,
 307 specific humidity, vapour pressure and NDVI lead to a positive change in ET (Figure 4 a, b, e, f, &
 308 i). In contrast, a positive change in mean temperature, windspeed, and AED leads to a decline in ET
 309 (Figure 4 c, d, & h). Among the climatic variables, vapour pressure has the strongest positive Pearson
 310 correlation coefficient ($r=0.67$, $p<0.05$) while mean temperature, windspeed and AED have the
 311 strongest negative Pearson correlation coefficients ($r>-0.70$, $p<0.05$) with ET.



312
 313 Figure 5: Response of ET to climate and environmental factors: (a) precipitation, (b) soil moisture,
 314 (c) mean temperature (d) windspeed, (d) net radiation, (f) specific humidity, (g) vapour pressure, (h)
 315 AED and (i) NDVI. Each dot in the plot denotes a watershed.

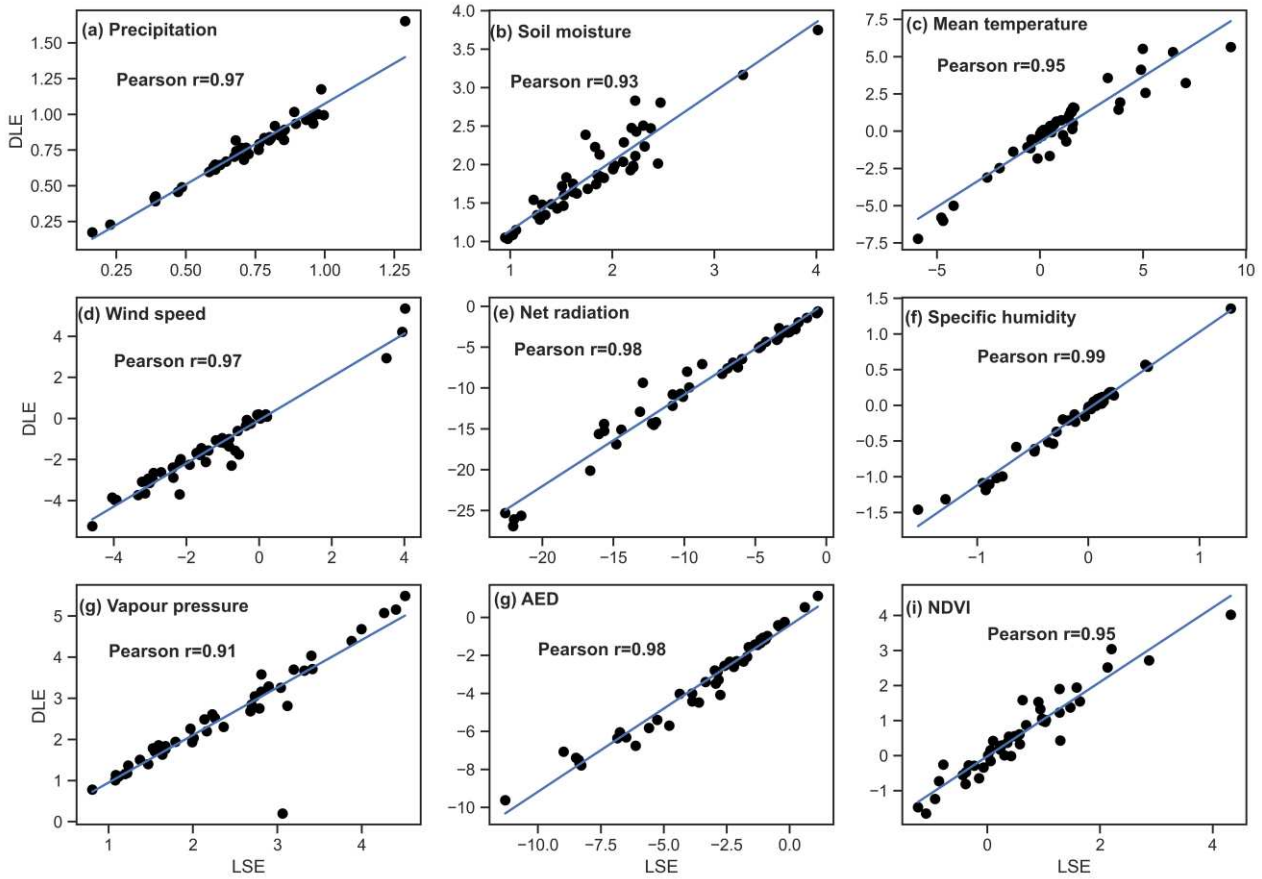
316

317

318

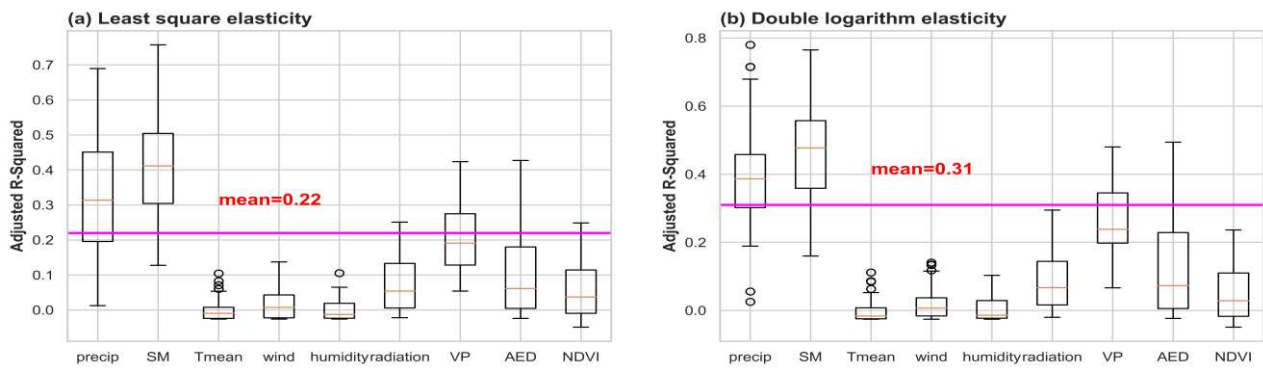
319 **3.3. Quantifying the effects of climate and vegetation changes on ET**

320 The LSE and DLE models were used to calculate the elasticity coefficients of the independent
321 variables on ET. Results of the Pearson correlation between the elasticity coefficients from both
322 models are shown in Figure 6.



323
324 **Figure 6:** Relationship between elasticity coefficients produced by both models. DLE: double
325 logarithm elasticity and LSE: least square elasticity.

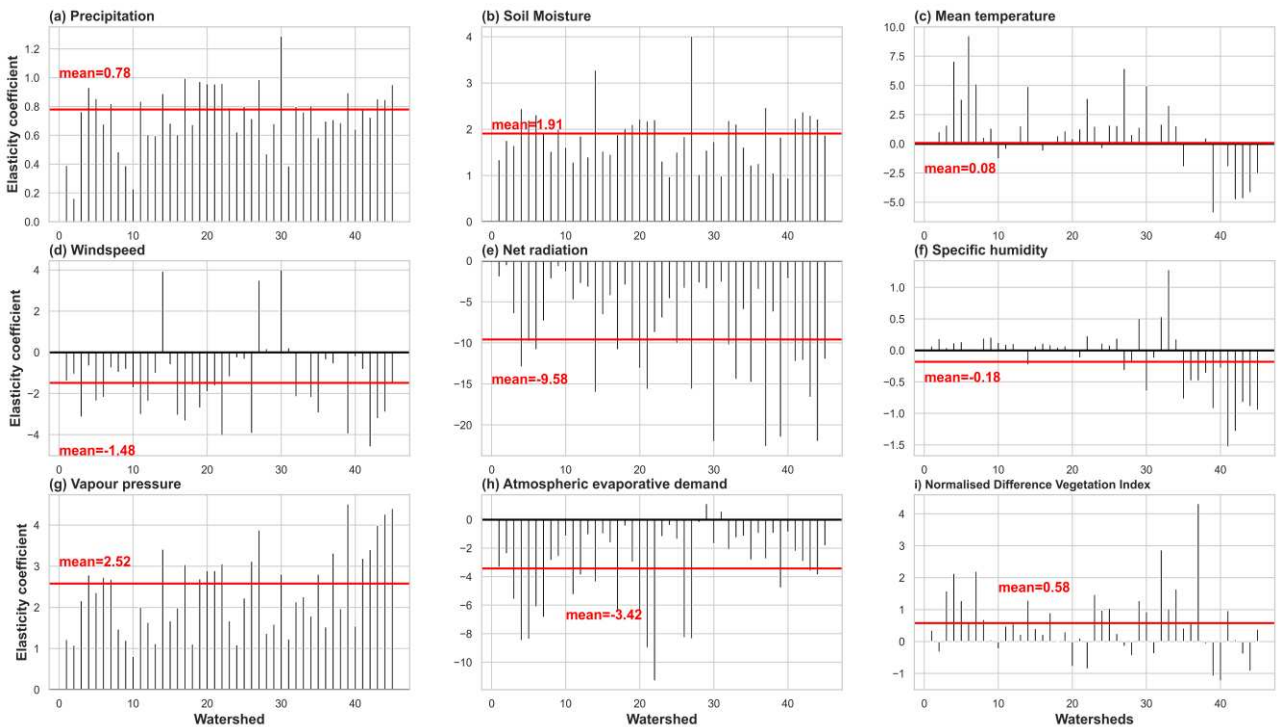
326 Pearson correlation coefficients between the elasticity coefficients produced by both models are
327 substantially high ($r > 0.91$, $p < 0.05$) for all variables suggesting that both models have similar
328 performance (Figure 6). To determine which of the models to be adopted for further analyses, we
329 used the adjusted R^2 values obtained from the linear regression analysis between ET and the different
330 independent variables, and their log-transformed counterparts as explained in the methods section.
331 Adjusted R^2 values obtained from LSE and DLE models are available in Figure 7 for all the
332 watersheds.



333

334 Figure 7: Comparison of adjusted R^2 values using the LSE and DLE models for all the watersheds
 335 in the Sahel. Precip: precipitation; SM: soil moisture; VP: vapour pressure, AED: atmospheric
 336 evaporative demand; NDVI: normalised difference vegetation index. The horizontal magenta-
 337 coloured lines represent the mean adjusted R^2 obtained using each method while the values in red
 338 represent the mean adjusted R^2 for all watersheds.

339 Analyses indicate that the mean adjusted R^2 from the DLE model is (0.31) while that from the LSE
 340 is (0.22) (Figure 7). Since the adjusted R^2 from DLE is higher than that of LSE, the elasticity
 341 coefficients from DLE are presented and discussed throughout the rest of this paper.



342

343 Figure 8: Elasticity coefficients of the independent variables on ET in all the watersheds in the Sahel.
 344 Each vertical line represents a watershed while the red horizontal line is the mean elasticity
 345 coefficient value for all the watersheds. The values in red are mean elasticity coefficients.

346 Figure 8 shows the elasticity coefficients of climate and environmental factors on ET. Results from
347 the analyses show that precipitation, soil moisture, and vapour pressure produced positive elasticity
348 coefficients on ET across all the watersheds while mean temperature and NDVI produced positive
349 elasticity coefficients in about 80% of the watersheds (Figure 8a, b, g & i). Other independent
350 variables produce mixed scores (positive and negative elasticity coefficients) across the watersheds.
351 Elasticity coefficients range from (0.17 to 165), (1.03 to 3.75), (8.55 to -5.65), (-5.25 to 5.35), (-
352 26.92 to -0.61), (1.46 to 1.36), (0.19 to 5.49), (-9.92 to 1.13) and (-1.65 to 4.09) with corresponding
353 means of 0.78, 1.90, 0.08, -1.48, -9.58, -0.18, 2.52, -3.41, & 0.57 for precipitation, soil moisture,
354 mean temperature, windspeed, net radiation, specific humidity, vapour pressure, AED and NDVI,
355 respectively. Elasticity coefficients obtained suggest that climatic factors produced higher elasticity
356 coefficients on ET than environmental factors (Figure 8). Furthermore, vapour pressure has a greater
357 positive influence on ET than soil moisture and precipitation (Figure 8a, b & g). Conversely, net
358 radiation shows a greater negative effect on ET compared to other climate variables (Figure 8e).

359 **4. Discussion**

360 **4.1. Mean annual estimates.**

361 Generally, higher AED values recorded around the central Sahel may be attributed to higher mean
362 temperature, windspeed, net radiation and vapour pressure which all have different modulating
363 effects on AED. On the other hand, higher NDVI values observed in watersheds around the southern
364 fringes of the Sahel may be attributed to higher annual precipitation and soil moisture availability.

365 **4.2. Trend analysis**

366 The results of trend analysis are consistent with those from other studies around the Sahel. For
367 example, Ndehedehe *et al.* (2018) and Adeyeri and Ishola (2021) found increasing trends in annual
368 ET across the western and central Sahel using data derived from MODIS and GLEAM respectively.
369 Using reanalysis data obtained from the Modern-Era Retrospective analysis for Research and
370 Applications (MERRA), Ndiaye *et al.* (2020) also reported increasing trends in solar radiation, and
371 specific humidity and decreasing trends in windspeed in the western Sahel. Cook *et al.* (2022)

372 reported increasing trends in mean temperature across the Sahel, reduced (increased) windspeed in
373 the western (eastern) Sahel and increased specific humidity in the central Sahel and our analysis are
374 consistent with their results. Declining trends in ET in parts of the Sahel are also consistent with
375 results from a global study which attributed the decline to changes in specific humidity (Yang *et al.*,
376 2019). Increasing trends in precipitation and mean temperature follow results reported in several
377 studies in the region e.g., (Nkiaka *et al.*, 2017; Ilori and Ajayi, 2020; Dembélé *et al.*, 2022).
378 Increasing trends in annual precipitation in the Sahel have been attributed to changes in global
379 circulation patterns such as sea surface temperatures and increased moisture recycling in the region
380 (Yu *et al.*, 2017; Biasutti, 2019). Increasing mean annual temperature follow a global pattern that
381 has been attributed to global warming (Hegerl *et al.*, 2019). Decreasing trends in incoming solar
382 radiation around the central Sahel may be due to increasing precipitation which increases cloud
383 cover over the region which in-turn reduces incoming solar radiation at the surface (Giannini, 2010;
384 Cook *et al.*, 2022). Increasing specific humidity in parts of the Sahel have been attributed to
385 increasing surface temperatures and stronger monsoon winds carrying more moisture from the Gulf
386 of Guinea (Cook *et al.*, 2022). Increasing trends in AED parts of the Sahel reflect the increasing
387 trends in mean temperature in those areas which is also consistent with results from another study
388 in the region (Abiye *et al.*, 2019). Many studies in the Sahel attributed increasing trends in NDVI to
389 precipitation increase (Yu *et al.*, 2017; Ogutu *et al.*, 2021; Jiang *et al.*, 2022). However, there is a
390 strong spatial heterogeneity in the distribution of NDVI trends across the region. Overall, our
391 analyses suggest that increasing trends in annual ET across the Sahel may be attributed to different
392 climatic and environmental factors. This is the first study to assess the effects of vegetation cover
393 on ET in the Sahel and as the GGWI is still under implementation, it not yet known how increasing
394 tree cover in the Sahel will affect the vegetation-hydrology-climate interactions especially as the
395 trees become mature in the decades to come. As such, more studies are needed in the region to
396 understand vegetation-hydrology-climate interactions under different alternative scenarios.

397

398 4.3. Factors influencing ET.

399 4.3.1. Climatic (abiotic) factors

400 The study uses several climatic variables including precipitation, mean temperature, windspeed, net
401 radiation, specific humidity, vapour pressure and AED to assess the factors influencing ET
402 variability in the Sahel. The three statistical methods including PCC which considers the collinearity
403 and interactions among the different independent variables revealed that precipitation, vapour
404 pressure and humidity are climatic variables with the strongest influence on ET. Multivariable
405 regression analyses show that the climatic factors contribute about 75.11% of the ET variance with
406 mean temperature, windspeed, vapour pressure and AED contributing the highest to ET variance.
407 Results from our analyses are consistent with those from previous studies in the western Sahel
408 (Adeyeri and Ishola, 2021; Ndiaye *et al.*, 2021). Multivariable regression analyses also indicate that
409 mean temperature and windspeed have a greater negative influence on ET than AED because of
410 their higher relative contributions to ET variance. It is worth highlighting that AED reflects the
411 atmospheric drying power and is influenced by all the other climate variables except precipitation.
412 This implies that the different climate variables have varying modulating effects on AED which may
413 influence the relationship between ET and AED. Nevertheless, the strong negative Pearson
414 correlation between ET and AED suggest that there may be a complimentary relationship between
415 them as suggested in a previous study (Brutsaert, 2015). This has been attributed to the fact that
416 AED in dryland areas is higher than precipitation and ET combined, and as such, ET is limited by
417 water availability (Yang *et al.*, 2019).

418 Positive Pearson correlations between ET and precipitation, net radiation and specific
419 humidity and the negative relationship between ET and mean temperature and AED have also been
420 observed in other dryland regions e.g., (Li *et al.*, 2022). Precipitation is the main supplier of water
421 for ET consumption while net radiation provides the energy needed for ET to occur. The negative
422 correlation between mean temperature and ET may be attributed to rising global temperatures which

423 in-turn enhance soil moisture depletion leading to limited water for soil evaporation and vegetation
424 growth which both influence ET in water-limited environments (Jung *et al.*, 2010).

425 **4.3.2. Environmental (biotic) factors**

426 Results of our analyses indicate that biotic factors (soil moisture and NDVI) have less influence on
427 ET compared to abiotic factors (climatic variables) with a relative contribution of 24.79% to ET
428 variance. The PCC between ET and NDVI shows a weak score ($r=0.28$, $p<0.01$) even though
429 statistically significant at 1% significance level (Table 2). This is consistent with results obtained in
430 other dryland regions (Chen *et al.*, 2022; Zheng *et al.*, 2022). The low relative contribution of
431 vegetation cover to ET may be attributed to the fact that vegetation covers varies seasonally and also
432 depends on the characteristics of the vegetation structure such as leaf area index (LAI), root depth,
433 vegetation coverage, physiology, age and vegetation type e.g., forest, agriculture, or grassland
434 (Odongo *et al.*, 2019). The present study was conducted at an annual timescale which may mask the
435 strong seasonal correlations between ET and NDVI in the rainy season when ET is not limited by
436 water supply. Nevertheless, Pearson correlation between ET and NDVI shows that a positive change
437 in NDVI leads to a corresponding positive change in ET which is in-line with results from other
438 studies e.g., (Chen *et al.*, 2022; Zheng *et al.*, 2022). This suggest that as vegetation cover increases
439 in the Sahel, this may likely increase the rate of ET in the region. The low PCC score between ET
440 and soil moisture may be attributed to increasing global temperatures which depletes the amount of
441 soil moisture available for soil evaporation and transpiration.

442 **4.4. Quantitative attribution of ET change**

443 The impact of climate variability and vegetation change on ET in the Sahel was quantified using the
444 double logarithm elasticity model. Mean elasticity coefficients were 0.78, 1.90, 0.08, -1.48, -9.58, -
445 0.18, 2.52, -3.41, & 0.57 for precipitation, soil moisture, mean temperature, windspeed, net
446 radiation, specific humidity, vapour pressure, AED and NDVI, respectively. This implies that a 10%
447 increase in precipitation, soil moisture, mean temperature, vapour pressure and NDVI will increase
448 ET by approximately 8%, 19%, 0.8%, 25% & 6% respectively. Vapour pressure contributes

449 substantially to ET variance and also produced the highest positive elasticity coefficient on ET which
450 is consistent with results obtained from other dryland regions (Ma *et al.*, 2019). The greater positive
451 effect of vapour pressure on ET in water-limited environments may be attributed to the fact that this
452 variable can influence plant stomatal activity and canopy photosynthesis (Yang *et al.*, 2022). In
453 contrast, a 10% increase in windspeed, net radiation, and AED leads to a decline in ET by
454 approximately 15%, 95%, & 34%, respectively. This is consistent with results from another study
455 in the region which showed that net radiation, and mean temperature had a negative impact on ET
456 (Yang *et al.*, 2019). Vapour pressure, soil moisture, precipitation and NDVI produced the highest
457 positive elasticity coefficients while net radiation and AED had the highest negative elasticity
458 coefficients on ET.

459 NDVI also produced positive elasticity coefficients across most watersheds suggesting that
460 increasing vegetation greenness in the Sahel may enhance ET. However, increasing vegetation
461 greenness in the Sahel may lead to water scarcity as more water may be lost to the atmosphere
462 through the ET. Additional research is needed to investigate vegetation-hydrology-climate
463 interaction in the Sahel as suggested at the end of section 4.2 above. This is very crucial considering
464 that enhance vegetation greenness has been shown to exacerbate water scarcity in some regions
465 (Vicente-Serrano *et al.*, 2021).

466 Although results from previous studies reported that precipitation is the dominant climatic
467 factor controlling ET in many regions (Feng *et al.*, 2020; Yang *et al.*, 2022), results from the present
468 study show that soil moisture has a stronger positive effect on ET than precipitation with a higher
469 mean elasticity coefficient (1.91) compared to precipitation (0.78). Moreover, the Pearson
470 correlation coefficient between soil moisture and ET is stronger (0.51) than that between
471 precipitation and ET (0.38). Furthermore, soil moisture had a higher relative contribution (21.12%)
472 to ET variance compared to precipitation (4.61%). This is in-line with results from a previous study
473 showing stronger positive correlations between soil moisture and ET compared to precipitation
474 (Yinglan *et al.*, 2019). In contrast the PCC between soil moisture and ET is (0.06) when controlling

475 for precipitation and other variables. This suggests that although precipitation is the main source of
476 water supply for ET, it would appear that across the Sahel, most of the precipitation is lost through
477 infiltration into the soil and therefore contributes indirectly to ET through transpiration (Yang *et al.*,
478 2019; Wang *et al.*, 2020). In fact, several studies have attributed the decline in ET in many areas to
479 limited soil moisture, thereby highlighting the fact that soil moisture is an important variable driving
480 ET in many regions (Jung *et al.*, 2010; Ndehedehe *et al.*, 2018; Zhou *et al.*, 2021). Furthermore,
481 moisture recycling in the Sahel has been identified as an important factor influencing ET in the
482 region (Yu *et al.*, 2017). Results of the different analyses conducted in this study suggest that the
483 mechanisms controlling ET variability in the Sahel are complex and could transcend natural climate
484 variability and vegetation change.

485 Whilst all the datasets used in the study have been validated and used extensively in previous
486 studies in the Sahel, we wish to acknowledge that satellite-derived and reanalysis data have inherent
487 uncertainties which may influence the results of the analyses reported in this study. Therefore, we
488 wish to caution that results from this study should be regarded with a bit of caution. We also wish
489 to acknowledge that the number of climatic and environmental factors analysed in the study are non-
490 exhaustive. However, the different factors are selected based on the results from previous studies
491 conducted around the world and in other dryland regions as highlighted in the introduction section
492 of this article. We acknowledge that there may be other important factors that may have been
493 inadvertently left out which could influence the results of the analyses reported herein which is
494 another weakness of the study.

495 **5. Conclusions**

496 The present study used analytical methods to assess the effects of climate and environmental changes
497 on ET in the Sahel over the period (1981-2021) for climate variables and (2000-2021) for vegetation
498 cover change. Results from our analyses show increasing trends in annual ET in the western, central
499 and parts of the eastern Sahel. Precipitation, soil moisture, mean temperature, and NDVI also show
500 increasing trends across the whole region while the other variables show both increasing and

501 decreasing trends in the different watersheds with a strong spatial heterogeneity in trend magnitudes.
502 Multivariable regression analyses show that both climatic and environmental factors contribute
503 about 80% of the ET variance. However, the relative contribution of climatic variables is 75.11%
504 while that of environmental variables is 24.71%. Vapour pressure had the highest mean positive
505 elasticity coefficient (2.58) while net radiation had the highest mean negative elasticity coefficient
506 (-9.58) on ET. Taking together, results from the different analyses carried out in the present study
507 suggest that the mechanisms controlling ET variability in the Sahel are complex and may transcend
508 climate and environmental changes. The LSE and DLE models produced similar elasticity
509 coefficients with strong Pearson correlations coefficients (>0.91) between the elasticity coefficients
510 from both models. This suggest that both models may be used to quantify the impact of climate
511 variability and vegetation change on ET in other regions. Results from the present results may be
512 crucial for adopting climate-smart reforestation policies and enhance water resources management
513 in Sahel. This is the first study to assess the effects of vegetation cover on ET in the Sahel. As the
514 GGWI is still ongoing, it not yet fully known how increasing tree cover will affect the vegetation-
515 hydrology-climate interactions especially as the trees become mature in the decades to come.
516 Therefore, more studies are needed in the region to disentangle the relationship between vegetation-
517 hydrology-climate under different alternative scenarios.

518

519

520

521

522

523

524

525

526

527 **Declaration of Competing Interest**

528 The authors declare that they have no known competing financial interests or personal relationships
529 that could have appeared to influence the work reported in this paper.

530 **Data availability statement:**

531 All data used to perform the analyses reported in this paper are freely available for download through
532 the Climate Engine Research App [<https://app.climateengine.com>] through a custom user account.

533 Shapefiles for the major basins and their sub-basins are freely available at
534 www.hydrosheds.org/hydrosheds-v2. Soil moisture data from GLEAM are freely available for
535 download at <https://www.gleam.eu/>.

536 **CRedit authorship contribution statement:**

537 **Elias Nkiaka:** Conceptualization, Data Curation, Methodology, Investigation, Resources, Writing-
538 Review & Editing, Funding acquisition.

539 **Robert G. Bryant:** Methodology, Investigation, Writing-Review & Editing.

540 **Moctar Dembélé:** Investigation, Writing-Review & Editing.

541 **Roland Yonaba:** Investigation, Writing-Review & Editing.

542 **Aigbedion Imuwahen Priscilla:** Writing-Review & Editing

543 **Harouna Karambiri:** Investigation, Writing-Review & Editing.

544 **Acknowledgements:**

545 Elias Nkiaka is funded by the Leverhulme Trust Early Career Fellowship, Grant/Award Number:
546 ECF-097-2020.

547

548

549

550

551

552

553

554

555 **Appendix A: Characteristics of the watersheds in the Sahelian belt**

Major Basin	Sub-basin	Number	Area (km ²)	Major Basin	Sub-basin	Number	Area (km ²)
Senegal	Bakoy	1	101,792	Lake	Bahr Azum	28	77,960
	Faleme	2	29,880	Chad	Bouluo	29	31,407
	Ferlo	3	45,131		Dillia	30	162,385
	Karakoro	4	47,574		Fitri	31	143,576
	Kolinbine	5	124,013		Komadugu Yobe	32	33,318
	Senegal 1	6	30,152		Komadugu Yobe	33	97,568
	Senegal 2	7	43,436	Koramas	34	43,751	
	Senegal 3	8	4,094	Nile	Abu Hut	35	45,971
	Senegal 4	9	7,086		Al Ghallah	36	17,948
Volta	Nakambe	10	110,851		Al Malik	37	125,049
	Sourou	11	31,072		Bandah	38	129,875
Niger	Bani 1	12	18,610		Blue Nile 1	39	23,014
	Bunsuru	13	31,043		Gelha	40	90,900
	Dallol				Nahr Atbarah 1	41	25,088
	Maouri	14	71,197		Mereb Wenz	42	73,113
	Dallol				Wadi Atshan	43	33,722
	Bosso	15	541,267	White Nile 1	44	17,690	
	Faga	16	39,113	Red Sea	Nahr al Qash	45	66,346
	Gorouol	17	53,944				
	Niger 10	18	31,167				
	Niger 11	19	11,467				
	Niger 12	20	12,352				
	Niger 13	21	123,166				
	Niger 9	22	60,907				
	N' kaba	23	38,787				
	Rima	24	6,585				
	Tarka	25	48,140				
Tchegue	26	32,872					
Tilemsi	27	87,033					

556
557
558
559
560
561
562
563
564
565
566
567
568
569

570 **References**

- 571 Abatzoglou, J.T., Dobrowski, S.Z., Parks, S.A. & Hegewisch, K.C. (2018). TerraClimate, a high-
572 resolution global dataset of monthly climate and climatic water balance from 1958–2015.
573 *Scientific data*, 5, 1-12
- 574 Abiye, O.E., Matthew, O.J., Sunmonu, L.A. & Babatunde, O.A. (2019). Potential evapotranspiration
575 trends in West Africa from 1906 to 2015. *SN Applied Sciences*, 1, 1-14
- 576 Adeyeri, O.E. & Ishola, K.A. (2021). Variability and Trends of Actual Evapotranspiration over West
577 Africa: The Role of Environmental Drivers. *Agricultural and Forest Meteorology*, 308,
578 108574
- 579 Ahiablame, L., Sheshukov, A.Y., Rahmani, V. & Moriasi, D. (2017). Annual baseflow variations as
580 influenced by climate variability and agricultural land use change in the Missouri River
581 Basin. *Journal of hydrology*, 551, 188-202
- 582 Arneth, A., Olsson, L., Cowie, A., Erb, K.-H., Hurlbert, M., Kurz, W.A., . . . Rounsevell, M.D.A.
583 (2021). Restoring Degraded Lands. *Annual Review of Environment and Resources*, 46, 569-
584 599
- 585 Asante, P.A., Rahn, E., Zuidema, P.A., Rozendaal, D.M., van der Baan, M.E., Läderach, P., . . .
586 Anten, N.P. (2022). The cocoa yield gap in Ghana: A quantification and an analysis of factors
587 that could narrow the gap. *Agricultural Systems*, 201, 103473
- 588 Biasutti, M. (2019). Rainfall trends in the African Sahel: Characteristics, processes, and causes.
589 *Wiley Interdisciplinary Reviews: Climate Change*, 10, e591
- 590 Boogaard, H., Schubert, J., De Wit, A., Lazebnik, J., Hutjes, R., Van der Grijn, G. (2020).
591 Agrometeorological indicators from 1979 to present derived from reanalysis. Copernicus
592 Climate Change Service (C3S) Climate Data Store (CDS).
- 593 Brutsaert, W. (2015). A generalized complementary principle with physical constraints for land-
594 surface evaporation. *Water Resources Research*, 51, 8087-8093

595 Chen, P., Wang, S., Song, S., Wang, Y., Wang, Y., Gao, D. & Li, Z. (2022). Ecological restoration
596 intensifies evapotranspiration in the Kubuqi Desert. *Ecological Engineering*, 175, 106504

597 Condon, L.E., Atchley, A.L. & Maxwell, R.M. (2020). Evapotranspiration depletes groundwater
598 under warming over the contiguous United States. *Nature communications*, 11, 873

599 Cook, P., Black, E.C., Verhoef, A., Macdonald, D. & Sorensen, J. (2022). Projected increases in
600 potential groundwater recharge and reduced evapotranspiration under future climate
601 conditions in West Africa. *Journal of Hydrology: Regional Studies*, 41, 101076

602 Dai, A., Lamb, P.J., Trenberth, K.E., Hulme, M., Jones, P.D. & Xie, P. (2004). The recent Sahel
603 drought is real. *International Journal of Climatology: A Journal of the Royal Meteorological*
604 *Society*, 24, 1323-1331

605 Dembélé, M., Schaeffli, B., van de Giesen, N. & Mariéthoz, G. (2020). Suitability of 17 rainfall and
606 temperature gridded datasets for largescale hydrological modelling in West Africa.
607 *Hydrology and Earth System Sciences Discussions*, 2020, 1-39

608 Dembélé, M., Vrac, M., Ceperley, N., Zwart, S.J., Larsen, J., Dadson, S.J., . . . Schaeffli, B. (2022).
609 Contrasting changes in hydrological processes of the Volta River basin under global
610 warming. *Hydrology and earth system sciences*, 26, 1481-1506

611 Dey, P. & Mishra, A. (2017). Separating the impacts of climate change and human activities on
612 streamflow: A review of methodologies and critical assumptions. *Journal of Hydrology*, 548,
613 278-290

614 Didan, K. (2015). MOD13A1 MODIS/Terra Vegetation Indices 16-Day L3 Global 500m SIN Grid
615 V006. *NASA EOSDIS Land Processes DAAC*, 10

616 Engström, A. & Ekman, A.M. (2010). Impact of meteorological factors on the correlation between
617 aerosol optical depth and cloud fraction. *Geophysical Research Letters*, 37

618 Feng, S., Liu, J., Zhang, Q., Zhang, Y., Singh, V.P., Gu, X. & Sun, P. (2020). A global quantitation
619 of factors affecting evapotranspiration variability. *Journal of Hydrology*, 584, 124688

620 Fensholt, R., Rasmussen, K., Nielsen, T.T. & Mbow, C. (2009). Evaluation of earth observation
621 based long term vegetation trends — Intercomparing NDVI time series trend analysis
622 consistency of Sahel from AVHRR GIMMS, Terra MODIS and SPOT VGT data. *Remote*
623 *Sensing of Environment*, 113, 1886-1898

624 Funk, C., Peterson, P., Landsfeld, M., Pedreros, D., Verdin, J., Shukla, S., . . . Hoell, A. (2015). The
625 climate hazards infrared precipitation with stations—a new environmental record for
626 monitoring extremes. *Scientific data*, 2, 1-21

627 Gbohoui, Y.P., Paturel, J.-E., Tazen, F., Mounirou, L.A., Yonaba, R., Karambiri, H. & Yacouba, H.
628 (2021). Impacts of climate and environmental changes on water resources: A multi-scale
629 study based on Nakanbé nested watersheds in West African Sahel. *Journal of Hydrology:*
630 *Regional Studies*, 35, 100828

631 Gebrechorkos, S.H., Pan, M., Lin, P., Anghileri, D., Forsythe, N., Pritchard, D.M., . . . Sheffield, J.
632 (2022). Variability and changes in hydrological drought in the Volta Basin, West Africa.
633 *Journal of Hydrology: Regional Studies*, 42, 101143

634 Ghins, L., Madurga-Lopez, I.M., Yabe, K. & Marley, J. (2022). Environmental fragility in the Sahel.
635 Giannini, A. (2010). Mechanisms of climate change in the semiarid African Sahel: The local view.
636 *Journal of Climate*, 23, 743-756

637 Goffner, D., Sinare, H. & Gordon, L.J. (2019). The Great Green Wall for the Sahara and the Sahel
638 Initiative as an opportunity to enhance resilience in Sahelian landscapes and livelihoods.
639 *Regional Environmental Change*, 19, 1417-1428

640 Güçlü, Y.S. (2020). Improved visualization for trend analysis by comparing with classical Mann-
641 Kendall test and ITA. *Journal of Hydrology*, 584, 124674

642 Guo, D., Westra, S. & Maier, H.R. (2017). Impact of evapotranspiration process representation on
643 runoff projections from conceptual rainfall-runoff models. *Water Resources Research*, 53,
644 435-454

645 Hasan, E., Tarhule, A., Kirstetter, P.-E., Clark III, R. & Hong, Y. (2018). Runoff sensitivity to
646 climate change in the Nile River Basin. *Journal of hydrology*, 561, 312-321

647 Heerspink, B.P., Kendall, A.D., Coe, M.T. & Hyndman, D.W. (2020). Trends in streamflow,
648 evapotranspiration, and groundwater storage across the Amazon Basin linked to changing
649 precipitation and land cover. *Journal of Hydrology: Regional Studies*, 32, 100755

650 Hegerl, G.C., Brönnimann, S., Cowan, T., Friedman, A.R., Hawkins, E., Iles, C., . . . Undorf, S.
651 (2019). Causes of climate change over the historical record. *Environmental Research Letters*,
652 14, 123006

653 Hernández, C.M., Faye, A., Ly, M.O., Stewart, Z.P., Vara Prasad, P., Bastos, L.M., . . . Ciampitti,
654 I.A. (2021). Soil and Climate Characterization to Define Environments for Summer Crops
655 in Senegal. *Sustainability*, 13, 11739

656 Ilori, O.W. & Ajayi, V.O. (2020). Change Detection and Trend Analysis of Future Temperature and
657 Rainfall over West Africa. *Earth Systems and Environment*, 4, 493-512

658 Jiang, M., Jia, L., Menenti, M. & Zeng, Y. (2022). Understanding spatial patterns in the drivers of
659 greenness trends in the Sahel-Sudano-Guinean region. *Big Earth Data*, 1-20

660 Jung, M., Reichstein, M., Ciais, P., Seneviratne, S.I., Sheffield, J., Goulden, M.L., . . . De Jeu, R.
661 (2010). Recent decline in the global land evapotranspiration trend due to limited moisture
662 supply. *Nature*, 467, 951-954

663 Khan, Z., Khan, F.A., Khan, A.U., Hussain, I., Khan, A., Shah, L.A., . . . Dyczko, A. (2022).
664 Climate-Streamflow Relationship and Consequences of Its Instability in Large Rivers of
665 Pakistan: An Elasticity Perspective. *Water*, 14, 2033

666 Lehner, B. & Grill, G. (2013). Global river hydrography and network routing: baseline data and new
667 approaches to study the world's large river systems. *Hydrological Processes*, 27, 2171-2186

668 Leroux, L., Bégué, A., Seen, D.L., Jolivot, A. & Kayitakire, F. (2017). Driving forces of recent
669 vegetation changes in the Sahel: Lessons learned from regional and local level analyses.
670 *Remote Sensing of Environment*, 191, 38-54

671 Li, S., Wang, G., Zhu, C., Lu, J., Ullah, W., Hagan, D.F.T., . . . Peng, J. (2022). Attribution of global
672 evapotranspiration trends based on the Budyko framework. *Hydrology and Earth System
673 Sciences*, 26, 3691-3707

674 Li, T., Xia, J., Zhang, L., She, D., Wang, G. & Cheng, L. (2021). An improved complementary
675 relationship for estimating evapotranspiration attributed to climate change and revegetation
676 in the Loess Plateau, China. *Journal of Hydrology*, 592, 125516

677 Ma, Z., Yan, N., Wu, B., Stein, A., Zhu, W. & Zeng, H. (2019). Variation in actual
678 evapotranspiration following changes in climate and vegetation cover during an ecological
679 restoration period (2000–2015) in the Loess Plateau, China. *Science of the total environment*,
680 689, 534-545

681 Martens, B., Miralles, D.G., Lievens, H., Van Der Schalie, R., De Jeu, R.A., Fernández-Prieto, D.,
682 . . . Verhoest, N.E. (2017). GLEAM v3: Satellite-based land evaporation and root-zone soil
683 moisture. *Geoscientific Model Development*, 10, 1903-1925

684 Mbow, C. (2017). *The Great Green Wall in the Sahel*. Oxford University Press.

685 Mbow, H.-O.P., Reisinger, A., Canadell, J. & O'Brien, P. (2017). Special Report on climate change,
686 desertification, land degradation, sustainable land management, food security, and
687 greenhouse gas fluxes in terrestrial ecosystems (SR2). *Ginevra, IPCC*, 650

688 Ndehedehe, C.E., Okwuashi, O., Ferreira, V.G. & Agutu, N.O. (2018). Exploring evapotranspiration
689 dynamics over sub-Saharan Africa (2000–2014). *Environmental monitoring and assessment*,
690 190, 1-19

691 Ndiaye, P.M., Bodian, A., Diop, L., Dezetter, A., Guilpart, E., Deme, A. & Ogilvie, A. (2021).
692 Future trend and sensitivity analysis of evapotranspiration in the Senegal River Basin.
693 *Journal of Hydrology: Regional Studies*, 35, 100820

694 Nicholson, S.E., Tucker, C.J. & Ba, M. (1998). Desertification, drought, and surface vegetation: An
695 example from the West African Sahel. *Bulletin of the American Meteorological Society*, 79,
696 815-830

697 Nkiaka, E., Bryant, R.G. & Kom, Z. (2024). Understanding Links Between Water Scarcity and
698 Violent Conflicts in the Sahel and Lake Chad Basin Using the Water Footprint Concept.
699 *Earth's Future*, 12, e2023EF004013

700 Nkiaka, E., Bryant, R.G., Ntajal, J. & Biao, E.I. (2022). Evaluating the accuracy of gridded water
701 resources reanalysis and evapotranspiration products for assessing water security in poorly
702 gauged basins. *Hydrol. Earth Syst. Sci.*, 26, 5899-5916

703 Nkiaka, E., Nawaz, N.R. & Lovett, J.C. (2017). Analysis of rainfall variability in the Logone
704 catchment, Lake Chad basin. *International Journal of Climatology*, 37, 3553-3564

705 Nkiaka, E. & Okafor, G.C. (2024). Changes in climate, vegetation cover and vegetation composition
706 affect runoff generation in the Gulf of Guinea Basin. *Hydrological Processes*, 38, e15124

707 Odongo, V.O., van Oel, P.R., van der Tol, C. & Su, Z. (2019). Impact of land use and land cover
708 transitions and climate on evapotranspiration in the Lake Naivasha Basin, Kenya. *Science of
709 the total environment*, 682, 19-30

710 Ogutu, B.O., D'Adamo, F. & Dash, J. (2021). Impact of vegetation greening on carbon and water
711 cycle in the African Sahel-Sudano-Guinean region. *Global and Planetary Change*, 202,
712 103524

713 Saha, S., Moorthi, S., Wu, X., Wang, J., Nadiga, S., Tripp, P., . . . Iredell, M. (2014). The NCEP
714 climate forecast system version 2. *Journal of climate*, 27, 2185-2208

715 Sankarasubramanian, A., Vogel, R.M. & Limbrunner, J.F. (2001). Climate elasticity of streamflow
716 in the United States. *Water Resources Research*, 37, 1771-1781

717 Schulze, K., Malek, Ž. & Verburg, P.H. (2021). How will land degradation neutrality change future
718 land system patterns? A scenario simulation study. *Environmental Science & Policy*, 124,
719 254-266

720 Sheffield, J., Wood, E.F., Pan, M., Beck, H., Coccia, G., Serrat-Capdevila, A. & Verbist, K. (2018).
721 Satellite remote sensing for water resources management: Potential for supporting
722 sustainable development in data-poor regions. *Water Resources Research*, 54, 9724-9758

723 Sun, C., Feng, X., Fu, B. & Ma, S. (2023). Desertification vulnerability under accelerated dryland
724 expansion. *Land Degradation & Development*, 34, 1991-2004

725 Tan, X., Liu, B. & Tan, X. (2020). Global changes in baseflow under the impacts of changing climate
726 and vegetation. *Water Resources Research*, 56, e2020WR027349

727 Teuling, A.J., De Badts, E.A., Jansen, F.A., Fuchs, R., Buitink, J., Hoek van Dijke, A.J. & Sterling,
728 S.M. (2019). Climate change, reforestation/afforestation, and urbanization impacts on
729 evapotranspiration and streamflow in Europe. *Hydrology and Earth System Sciences*, 23,
730 3631-3652

731 Tsai, Y. (2017). The multivariate climatic and anthropogenic elasticity of streamflow in the Eastern
732 United States. *Journal of Hydrology: Regional Studies*, 9, 199-215

733 Vicente-Serrano, S.M., Domínguez-Castro, F., Murphy, C., Peña-Angulo, D., Tomas-Burguera, M.,
734 Noguera, I., . . . Eklundh, L. (2021). Increased vegetation in mountainous headwaters
735 amplifies water stress during dry periods. *Geophysical Research Letters*, 48,
736 e2021GL094672

737 Wang, F., Notaro, M., Yu, Y. & Mao, J. (2023). Deficient precipitation sensitivity to Sahel land
738 surface forcings among CMIP5 models. *International Journal of Climatology*, 43, 99-122

739 Wang, L., Li, M., Wang, J., Li, X. & Wang, L. (2020). An analytical reductionist framework to
740 separate the effects of climate change and human activities on variation in water use
741 efficiency. *Science of the Total Environment*, 727, 138306

742 Yang, L., Feng, Q., Adamowski, J.F., Alizadeh, M.R., Yin, Z., Wen, X. & Zhu, M. (2021). The role
743 of climate change and vegetation greening on the variation of terrestrial evapotranspiration
744 in northwest China's Qilian Mountains. *Science of The Total Environment*, 759, 143532

745 Yang, L., Feng, Q., Zhu, M., Wang, L., Alizadeh, M.R., Adamowski, J.F., . . . Yin, Z. (2022).
746 Variation in actual evapotranspiration and its ties to climate change and vegetation dynamics
747 in northwest China. *Journal of Hydrology*, 607, 127533

748 Yang, Z., Zhang, Q., Hao, X. & Yue, P. (2019). Changes in evapotranspiration over global semiarid
749 regions 1984–2013. *Journal of Geophysical Research: Atmospheres*, 124, 2946-2963

750 Yinglan, A., Wang, G., Liu, T., Xue, B. & Kuczera, G. (2019). Spatial variation of correlations
751 between vertical soil water and evapotranspiration and their controlling factors in a semi-
752 arid region. *Journal of Hydrology*, 574, 53-63

753 Yu, Y., Notaro, M., Wang, F., Mao, J., Shi, X. & Wei, Y. (2017). Observed positive vegetation-
754 rainfall feedbacks in the Sahel dominated by a moisture recycling mechanism. *Nature*
755 *Communications*, 8, 1873

756 Zhang, Y., Kong, D., Gan, R., Chiew, F.H., McVicar, T.R., Zhang, Q. & Yang, Y. (2019). Coupled
757 estimation of 500 m and 8-day resolution global evapotranspiration and gross primary
758 production in 2002–2017. *Remote sensing of environment*, 222, 165-182

759 Zhang, Y., Zheng, H., Zhang, X., Leung, L.R., Liu, C., Zheng, C., . . . Kong, D. (2023). Future
760 global streamflow declines are probably more severe than previously estimated. *Nature*
761 *Water*, 1-11

762 Zheng, H., Miao, C., Li, X., Kong, D., Gou, J., Wu, J. & Zhang, S. (2022). Effects of vegetation
763 changes and multiple environmental factors on evapotranspiration across China over the past
764 34 years. *Earth's Future*, 10, e2021EF002564

765 Zheng, H., Zhang, L., Zhu, R., Liu, C., Sato, Y. & Fukushima, Y. (2009). Responses of streamflow
766 to climate and land surface change in the headwaters of the Yellow River Basin. *Water*
767 *resources research*, 45

768 Zhou, S., Williams, A.P., Lintner, B.R., Berg, A.M., Zhang, Y., Keenan, T.F., . . . Gentile, P. (2021).
769 Soil moisture–atmosphere feedbacks mitigate declining water availability in drylands.
770 *Nature Climate Change*, 11, 38-44

771